# FTIR Spectroscopy of the All-Trans Form of *Anabaena* Sensory Rhodopsin at 77 K: Hydrogen Bond of a Water between the Schiff Base and Asp75[†]

Yuji Furutani,[‡,§,||] Akira Kawanabe,[‡] Kwang-Hwan Jung,[⊥] and Hideki Kandori*[,‡,||]

*Department of Materials Science and Engineering, Nagoya Institute of Technology, Showa-ku, Nagoya 466-8555, Japan, Department of Biophysics, Graduate School of Science, Kyoto University, Sakyo-ku, Kyoto 606-8502, Japan, Core Research for Evolutional Science and Technology (CREST), Japan Science and Technology Corporation, Kyoto 606-8502, Japan, Department of Life Science and Interdisciplinary Program of Integrated Biotechnology, Sogang University, Shinsu-Dong 1, Mapo-Gu, Seoul 121-742, Korea*

*Received May 5, 2005; Revised Manuscript Received June 28, 2005*

ABSTRACT: *Anabaena* sensory rhodopsin (ASR) is an archaeal-type rhodopsin found in eubacteria, and is believed to function as a photosensor interacting with a 14 kDa soluble protein. Most of the residues in the retinal binding pocket are similar in ASR except proline 206, where the corresponding amino acid in other archaeal-type rhodopsins is highly conserved aspartate that constitutes the counterion complex of the positively charged protonated Schiff base. The recently determined X-ray crystallographic structure of ASR revealed a water molecule between the Schiff base and Asp75 [Vogeley, L., Sineshchekov, O. A., Trivedi, V. D., Sasaki, J., Spudich, J. L., and Luecke, H. (2004) *Science 306,* 1390−1393], as well as the case for bacteriorhodopsin (BR), a typical transport rhodopsin working as a proton pump. In this study, we applied low-temperature Fourier transform infrared (FTIR) spectroscopy to the all-trans form of ASR at 77 K, and compared the local structure around the chromophore and their structural changes upon retinal photoisomerization with those of BR. The K intermediate minus ASR difference spectra were essentially similar to those for BR, indicating that photoisomerization yields formation of the distorted 13-cis form. In contrast, little amide I bands were observed for ASR. The presence of the proline-specific vibrational bands suggests that peptide backbone alterations are limited to the Pro206 moiety in the K state of ASR. The N−D stretching of the Schiff base is presumably located at 2163 (−) and 2125 (−) $cm^{-1}$ in ASR, suggesting that the hydrogen bonding strength of the Schiff base in ASR is similar to that in BR. A remarkable difference between ASR and BR was revealed from water bands. Although ASR possesses a bridged water molecule like BR, the O−D stretching of water molecules was observed only in the $>2500$ $cm^{-1}$ region for ASR. We interpreted that the weak hydrogen bond of the bridged water between the Schiff base and Asp75 originates from their geometry. Since ASR does not pump protons, our result supports the working hypothesis that the existence of strongly hydrogen bonded water molecules is essential for proton pumping activity in archaeal rhodopsins.

Four archaeal-type rhodopsins [bacteriorhodopsin (BR),[1] halorhodopsin (HR), sensory rhodopsin (SR, also called sensory rhodopsin I), and phoborhodopsin (pR, also called sensory rhodopsin II)] were discovered in the cytoplasmic membrane of *Halobacterium salinarum* (*1*, *2*). The former two rhodopsins (BR and HR) function as light-driven proton and chloride pumps, respectively, while the latter two rhodopsins (SR and pR) as photosensors responsible for attractive and repellent phototaxis, respectively. They have been extensively studied as model systems that convert light energy to chemical potential or environmental signal. Although such archaeal-type rhodopsins were believed to exist only in Archaea, the genome sequencing projects and the environmental genomics of the past six years have revealed that archaeal rhodopsins also exist in Eukarya and Eubacteria. In eukaryotes, archaeal rhodopsins were found in fungi (*3*), green algae (*4*, *5*), dinoflagellates (*6*), and cryptomonads (*7*). Eubacterial rhodopsins were found both in $\gamma$- and $\alpha$-proteobacteria (*8*, *9*) and in *Anabaena* (*Notstoc*) sp. PCC7120, a freshwater cyanobacterium (*10*), which was called *Anabaena* sensory rhodopsin (ASR).

The gene encoding ASR, which is a membrane protein of 261 residues (26 kDa), and a small gene encoding a soluble protein of 125 residues (14 kDa) are under the same promoter in a single operon (*10*). The opsin gene is expressed heterologously in *Escherichia coli*, and it bound all-trans retinal to form a pink pigment ($\lambda_{max} = 549$ nm, dark-adapted form) with a photochemical reaction cycle with a half-life

[†] This work was supported in part by grants from Japanese Ministry of Education, Culture, Sports, Science, and Technology to H.K. (15076202) and by Research Fellowships from the Japan Society for the Promotion of Science for Young Scientists to Y.F.

* To whom correspondence should be addressed. Phone and fax: 81-52-735-5207. E-mail: kandori@nitech.ac.jp.

[‡] Nagoya Institute of Technology.

[§] Kyoto University.

[||] Japan Science and Technology Corp.

[⊥] Sogang University.

[1] Abbreviations: BR, bacteriorhodopsin; DM, *n*-dodecyl $\beta$-D-maltoside; $\lambda_{max}$, maximum absorption wavelength; PC, L-$\alpha$-phosphatidylcholine; ASR, *Anabaena* sensory rhodopsin; *p*pR, *pharaonis* phoborhodopsin (also called *Natronomonas pharaonis* sensory rhodopsin II); HOOP, hydrogen-out-of-plane; PSB, protonated Schiff base.

10.1021/bi050841o CCC: $30.25 
Published on Web 08/25/2005

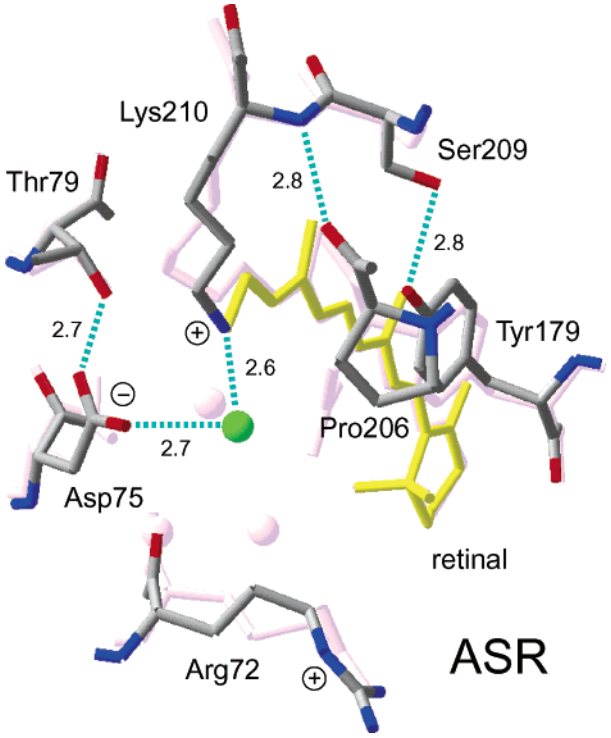


FIGURE 1: X-ray crystallographic structures of the Schiff base region of ASR and BR [PDB entries 1XIO (*11*) and 1C3W (*43*), respectively]. Each retinal molecule is fitted to compare the hydrogen bonding networks by using Swiss-PdbViewer (*48*). Top and bottom regions correspond to the cytoplasmic and extracellular sides, respectively. Green spheres (water 402) represent water molecules which form a hydrogen bond bridging the protonated Schiff base and its counterion, Asp75. Hydrogen bonds (blue dashed lines) are deduced from the structure, and the numbers are the hydrogen bond distances in angstroms.

of 110 ms (pH 6.8 and 18 °C) (*10*). The previous study reported that coexpression with the 14 kDa protein enhanced the rate of the photocycle, indicating physical interaction with ASR (*10*). This fact suggested that ASR works as a photosensory function instead of photoenergy production. According to the recently determined X-ray crystal structure (Figure 1), ASR accommodates both all-trans and 13-cis retinal in the ground state, which can be interconverted between them by illumination with blue (480 nm) or orange (590 nm) light (*11*). Such photochromic behavior is not observed in BR, HR, SR, and pR. These results might suggest that ASR is a photochromic color sensor.

Comparison of the amino acid sequences of ASR and BR shows that some important residues for the proton pump in BR are replaced in ASR (Figure 2). The proton donor to the Schiff base (Asp96 in BR) and one of proton release groups (Glu194 in BR) are replaced with serine residues, Ser86 and Ser188, respectively. These replacements are probably responsible for the slow photocycle of ASR on the analogy of *pharaonis* phoborhodopsin (*pp*R), whose corresponding residues are Phe86 and Pro183, respectively (*12*). Ten amino acid residues of 25 constituting the retinal binding site are different from those of BR, which probably yields a different absorption maximum and different photochromic behavior of ASR. Among them, the most interesting replacement in ASR is Pro206 at the corresponding position of Asp212 in BR. Asp212 constitutes a counterion complex of the Schiff base in BR, and the aspartate is highly conserved among archaeal rhodopsins. How is the hydrogen bonding network around the Schiff base modified in ASR by the presence of Pro206?

We have developed low-temperature Fourier transform infrared (FTIR) spectroscopy to detect X−H and X−D (X

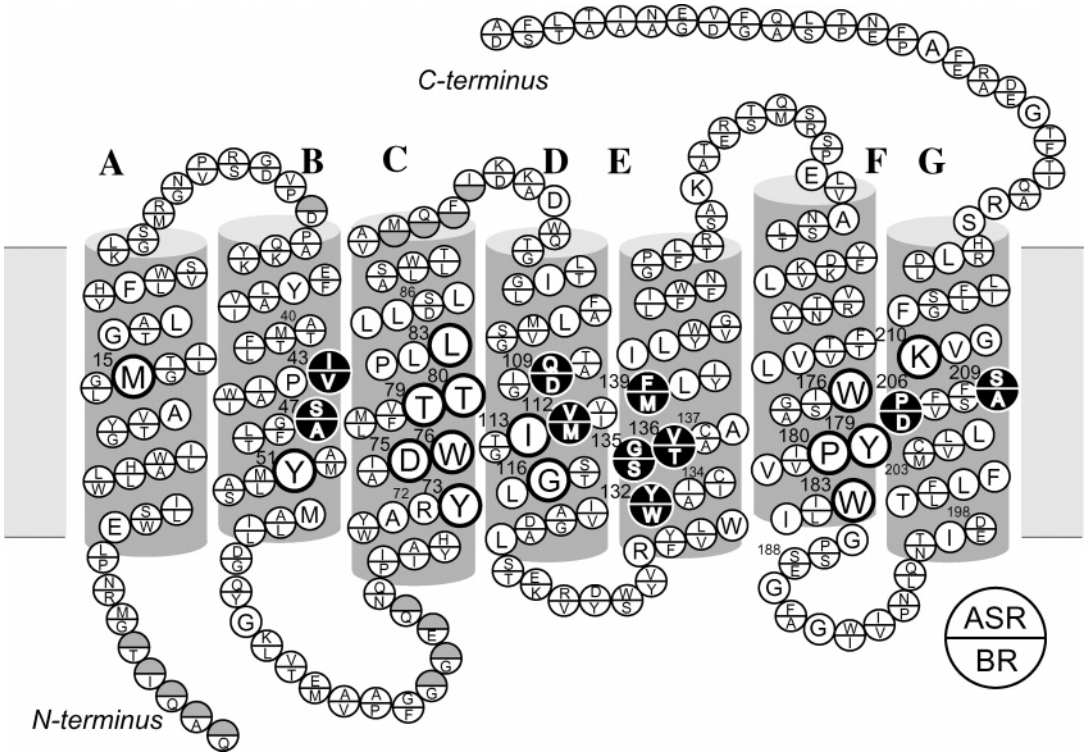


FIGURE 2: Comparison of the amino acid sequences of ASR and BR. The transmembrane topology is based on the crystallographic three-dimensional structure of BR. The sequence alignment was done using CLUSTAL W (*49*) with the default settings. Single letters in a circle denote residues common to ASR and BR. The residues that are different in ASR and BR are denoted at the top and bottom of the circles, respectively. The residues forming the retinal binding site within 5 Å of the chromophore are shown as bold or filled circles.

= O or N) stretching vibrations in the midinfrared region (4000−1800 $cm^{-1}$) (*13*, *14*). These vibrations are direct indications of the hydrogen bonding network, including internal water molecules. In fact, comparison of the K intermediate ($BR_K$) minus BR difference spectra between hydration with $D_2O$ and $D_2{}^{18}O$ in the X−D stretching region (2700−1800 $cm^{-1}$) enabled us to assign the O−D stretching vibrations of water molecules not only with a weak hydrogen bond (at >2500 $cm^{-1}$) but also with a strong hydrogen bond (at <2400 $cm^{-1}$). A mutation study showed that one of the O−D stretches (2171 $cm^{-1}$) originates from a bridge water molecule between the Schiff base and its counterion (Asp85) (*15*). Hydration switch of the water plays an important role in the proton transfer reaction in BR (*16*). In addition, interestingly, comprehensive studies of BR mutants and other rhodopsins have revealed that strongly hydrogen-bonded water molecules are only found in the proteins exhibiting proton pump activities (*17*). This suggests that a strongly hydrogen bonded water molecule that bridges the Schiff base and its counterion is essential for proton pumping. In terms of this idea, the FTIR study of ASR is intriguing, because ASR possesses a bridged water like BR (Figure 1), but does not pump protons (*10*).

In this study, we applied low-temperature FTIR spectroscopy to the all-trans form of ASR, and compared the difference spectra at 77 K with those of BR. The K intermediate minus ASR difference spectra show that the retinal isomerizes from the all-trans to the distorted 13-cis form like BR. The N−D stretching of the Schiff base was observed at 2163 (−) and 2125 (−) $cm^{-1}$, while the O−D stretchings of water molecules were observed in the >2500 $cm^{-1}$ region. These results indicate that the protonated Schiff base forms a strong hydrogen bond with a water molecule, which is connected to Asp75 with a weak hydrogen bond. This result with ASR supports our working hypothesis about the strong correlation between the proton pump activity and the existence of strongly hydrogen bonded water molecules in archaeal rhodopsins. In this article, we discuss the structural reason the bridged water molecule does not form a strong hydrogen bond in ASR.

## MATERIALS AND METHODS

*Sample Preparation of ASR.* Samples for this spectroscopic analysis were prepared as described previously (*10*, *18*). Briefly, *E. coli* strain BL21 (Stratagene) was transformed by introducing pMS107 derivative plasmids (*10*) which encode the *Anabaena* opsin and were grown in 2× YT medium in the presence of ampicillin (50 μg/mL) at 38 °C. Three hours after IPTG induction with 10 μM all-trans retinal, pink-colored cells were sonicated, solubilized with 1% DM, and purified with a $Ni^{2+}$−NTA column. The purified ASR protein was then reconstituted into PC liposomes by dialysis to remove the detergent with Bio-Beads, where the molar ratio of the added PC to ASR was 50:1.

The ASR protein in PC liposomes was washed three times with a buffer [2 mM sodium phosphate (pH 7.0)]. A 60 μL aliquot was deposited on a $BaF_2$ window 18 mm in diameter, and the sample was dried in a glass vessel that was evacuated with an aspirator.

*FTIR Spectroscopy.* FTIR spectroscopy was performed as described previously (*18*). Since the all-trans form is most abundant for the dark-adapted ASR (*11*), ASR films were kept in the dark for 3 days. Completely dark adapted ASR was hydrated with $H_2O$, $D_2O$, or $D_2{}^{18}O$ before measurements. Then, the sample was placed in a cryostat (DN-1704, Oxford) mounted on the cell for the FTIR spectrometer (FTS-40, Bio-Rad). The cryostat was equipped with a temperature controller (ITC-4, Oxford), and the temperature was regulated with 0.1 K precision. All the experimental procedures were performed in the dark or under dim red light (>670 nm) before the spectroscopic measurement.

Photoreactions of the all-trans and 13-cis forms strongly depend on the illumination wavelength of ASR. In this study, it is required that we reduce the extent of the photoreaction of the 13-cis form as much as possible. By using a maker band in the fingerprint (1200−1100 $cm^{-1}$) region (see the Results), we established the following illumination conditions at 77 K, where difference spectra depict the photoreaction of the 13-cis form at <20%. Illumination with 543 nm light at 77 K for 1 min converted ASR to $ASR_K$. $ASR_K$ was reconverted to ASR upon illumination with >590 nm light for 1 min, as evidenced by a mirror image of the difference spectra. Each difference spectrum was calculated from two spectra constructed from 128 interferograms taken before and after the illumination. Twenty-four ($H_2O$ and $D_2O$) or forty-eight ($D_2{}^{18}O$) difference spectra were obtained and averaged to produce the $ASR_K$ minus ASR spectrum. ASR molecules are randomly oriented in the liposome film, which is confirmed by linear dichroism experiments, so we did not apply dichroic measurements using an IR polarizer. The obtained difference spectra were compared with those for BR with the window tilting angle of 53.5° in the polarized measurement, where all vibrational bands are observed in the highly oriented BR molecule.

## RESULTS

In spectroscopic studies of archaeal rhodopsins, it is important to separate the photocycles of the all-trans from the 13-cis forms. In the case of BR, a well-known light adaptation procedure leads to a complete all-trans form. On the other hand, Vogeley et al. reported that ASR has a maximal amount of the all-trans form in the dark (>75%), while light adaptation rather decreases the amount of the all-trans form (*11*). It was reproduced in this study, and hence, we used the dark-adapted ASR sample. The absorption maximum of the all-trans enriched ASR was located at 549 nm, which was the same value reported previously (*11*). Low-temperature UV−visible spectroscopy of ASR showed that the red-shifted intermediate ($ASR_K$) is formed at 77 K. The difference absorption maximum was located at 593 nm, and we estimated the absolute absorption maximum of $ASR_K$ at 589 nm (data not shown).

*Comparison of the Difference Infrared Spectra Obtained by the Photoreactions of Anabaena Sensory Rhodopsin (ASR) at 77 K with Those of Bacteriorhodopsin (BR).* Figure 3 shows the $ASR_K$ minus ASR (a) and $BR_K$ minus BR spectra (b), which were measured at 77 K in the hydration with $H_2O$ (solid lines) and $D_2O$ (dotted lines). Unlike those of BR, the difference spectra of ASR contain a mixture from photoproducts of the all-trans and 13-cis form. However, we estimated that the contribution is less than 20% by use of the marker band (1178 $cm^{-1}$) under our illumination condi-

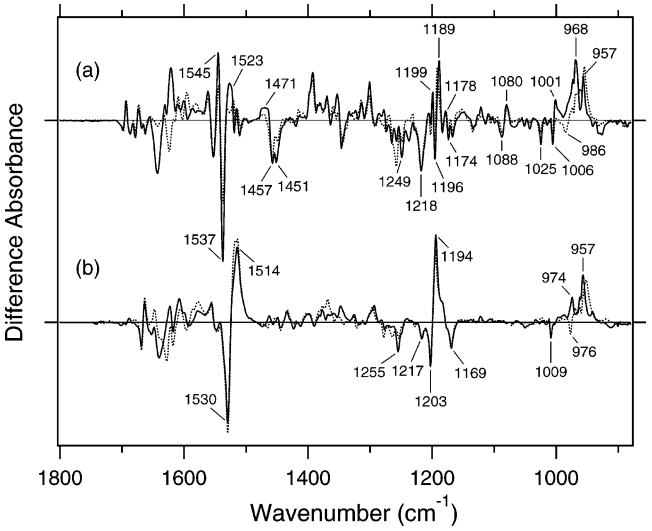


FIGURE 3: $ASR_K$ minus ASR (a) and $BR_K$ minus BR (b) spectra in the 1800−850 cm$^{-1}$ region measured at pH 7 and 77 K upon hydration with $H_2O$ (—) and $D_2O$ (•••), respectively. In the hydrated film, ASR molecules are oriented randomly, while BR molecules are highly oriented. The spectrum in panel b is reproduced from Kandori et al. (*50*), where the sample window is tilted by 53.5°. One division of the *y*-axis corresponds to 0.005 absorbance unit.

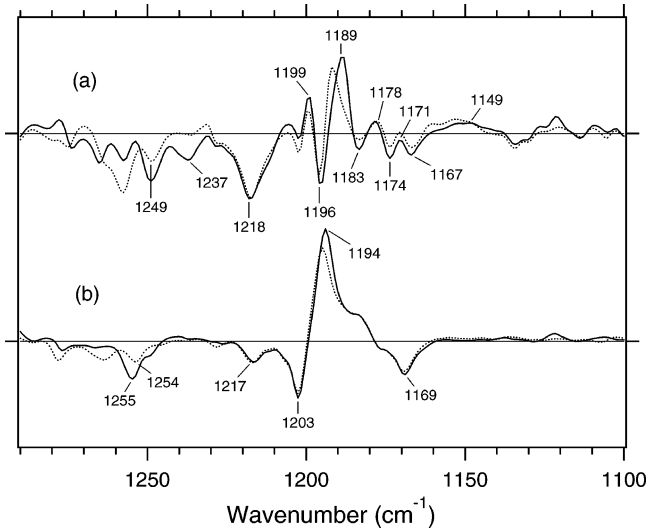


FIGURE 4: $ASR_K$ minus ASR (a) and $BR_K$ minus BR (b) spectra in the 1290−1100 cm$^{-1}$ region, which correspond to C−C stretching vibrations and N−H in-plane bending vibrations of the retinal chromophore. The sample was hydrated with $H_2O$ (—) or $D_2O$ (•••). One division of the *y*-axis corresponds to 0.004 absorbance unit.

tions (see below). All vibrational bands described in this article originate from the photoreaction of the all-trans form.

The negative band at 1537 cm$^{-1}$ corresponds to the ethylenic stretching vibration of the all-trans chromophore in ASR, which exhibits an absorption maximum at 549 nm (*11*). The frequency is in good agreement with the well-known linear correlation between the ethylenic stretching frequencies and absorption maxima for various retinal proteins (*19*). In the case of BR, the bands at 1530 (−)/1514 (+) cm$^{-1}$ correspond to the ethylenic stretching vibrations of the unphotolyzed and K intermediate ($BR_K$) states, respectively (Figure 3b). On the other hand, two positive bands appeared at 1545 and 1523 cm$^{-1}$ for ASR (Figure 3a). According to the linear correlation between the ethylenic stretching frequencies and absorption maxima (*19*), we predicted the ethylenic stretch of $ASR_K$ (589 nm) to be at 1525 cm$^{-1}$. Therefore, the 1523 cm$^{-1}$ band is likely to be the ethylenic band of $ASR_K$, and the band at 1545 cm$^{-1}$ can possibly be assigned to the amide II mode. A similar observation was gained for halorhodopsin (*20*), where the K intermediate exhibits two positive bands at 1538 and 1514 cm$^{-1}$ with a negative band at 1525 cm$^{-1}$.

Remarkable spectral differences between ASR and BR were seen in the 1500−1450 cm$^{-1}$ region. Two negative bands at 1457 and 1451 cm$^{-1}$ and a positive band at 1471 cm$^{-1}$ were observed for ASR (Figure 3a). Among these three bands, the 1457 cm$^{-1}$ band is insensitive to H−D exchange, whereas the bands at 1471 and 1451 cm$^{-1}$ reduce the half-intensity in $D_2O$. On the other hand, such strong bands are absent for BR (Figure 3b). This frequency region corresponds to the imide II vibrations of proline, and the assignment of these bands is now in progress.

*Comparison of the Vibrational Bands of the Retinal Chromophore between ASR and BR.* C−C stretching vibrations of the retinal in the 1250−1150 cm$^{-1}$ region are sensitive to the local structure of the chromophore. In Figure 4b, the negative bands at 1217, 1169, 1254, and 1203 cm$^{-1}$ were assigned to the C8−C9, C10−C11, C12−C13, and C14−C15 stretching vibrations of BR, respectively (*21*). These frequencies are characteristic of the all-trans retinal protonated Schiff base, though the frequencies are higher because of the charge delocalization of the retinal molecule in BR. Upon formation of $BR_K$, the retinal isomerizes to the 13-cis form, resulting in the appearance of a strong positive band at 1194 cm$^{-1}$, which is assigned to C10−C11 and C14−C15 stretching vibrations (*22*).

A more complex spectral feature was observed for ASR in the 1250−1150 cm$^{-1}$ region (Figure 4a). One reason is that the photoreaction of the 13-cis form to its photoproduct contributes to these spectra. It is known that a positive band at ∼1180 cm$^{-1}$ is a marker band of such a reaction in BR (*23*). Similarly, in this study for ASR, we found that the bands at 1183 (−)/1178 (+) cm$^{-1}$ increase in intensity when illumination wavelengths are changed. Thus, we interpreted that the bands originate from the photoreaction of the 13-cis form in ASR as well as in BR. In other words, we established the illumination conditions to maximally reduce the bands at 1183 (−)/1178 (+) cm$^{-1}$ in this study. The FTIR study of the 13-cis form will be published elsewhere.

In the case of the all-trans form of ASR, the negative bands at 1218, 1174 (and/or 1167), 1249, and 1196 cm$^{-1}$ were tentatively assigned to the C8−C9, C10−C11, C12−C13, and C14−C15 stretching vibrations, respectively (Figure 4a). These frequencies are similar to those of BR (each frequency difference is <10 cm$^{-1}$), supporting the fact that the retinal configuration of ASR in the dark-adapted state is all-trans. However, the relatively large difference in C12−C13 (6 cm$^{-1}$) and C14−C15 (7 cm$^{-1}$) stretching vibrations suggests that the retinal structure near the Schiff base region is somehow different in ASR and BR. In addition, the intensity of the band at 1218 cm$^{-1}$ is 3 times larger than that of BR, which also suggests different retinal structure around the C8−C9 bond. Upon formation of $ASR_K$, the retinal molecule is considered to isomerize to the 13-cis form in analogy to the case of BR. However, unlike BR, there are three positive

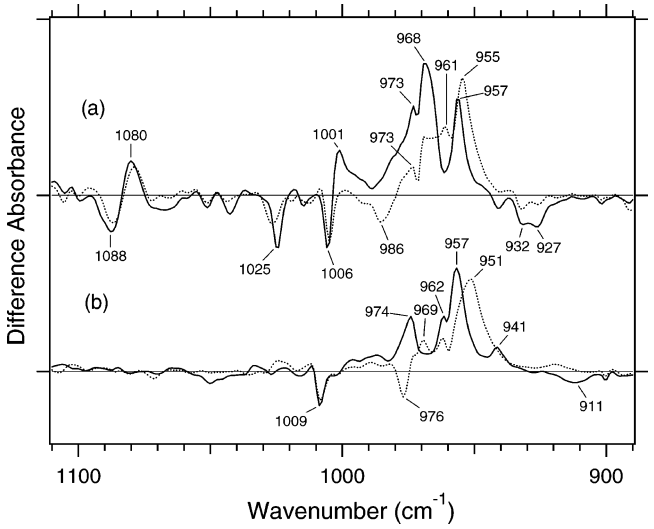


FIGURE 5: $ASR_K$ minus ASR (a) and $BR_K$ minus BR (b) spectra in the 1110−890 $cm^{-1}$ region, which correspond to hydrogen out-of-plane (HOOP) vibrations of the retinal chromophore The sample was hydrated with $H_2O$ (—) or $D_2O$ (•••). One division of the *y*-axis corresponds to 0.002 absorbance unit.

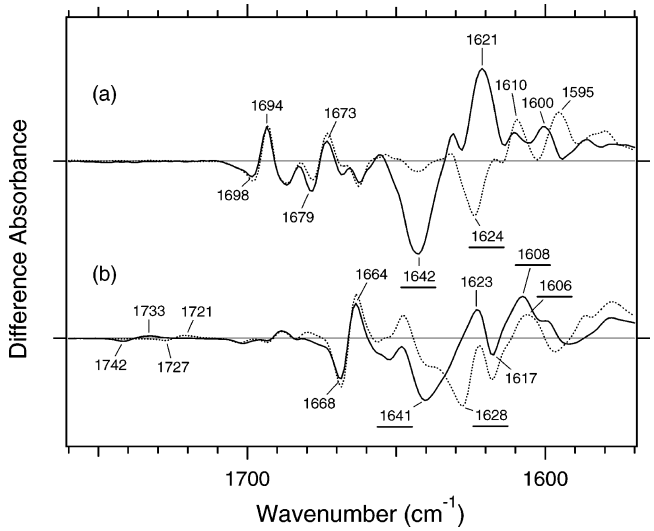


FIGURE 6: $ASR_K$ minus ASR (a) and $BR_K$ minus BR (b) spectra in the 1760−1570 $cm^{-1}$ region, most of which can be ascribed to vibrations of the protein moiety. The underlined peaks are C═N stretching vibrations of the chromophore. The sample was hydrated with $H_2O$ (—) or $D_2O$ (•••). One division of the *y*-axis corresponds to 0.003 absorbance unit.

bands at 1199, 1189, and 1149 $cm^{-1}$. The 1199 $cm^{-1}$ band is not sensitive to H−D exchange, suggesting the origin as a C−C stretching vibration in the polyene chain of the retinal molecule. The bands at 1189 and 1149 $cm^{-1}$ are upshifted upon hydration with $D_2O$, suggesting that they are influenced by the Schiff base vibration. The 1189 $cm^{-1}$ band can be assigned to the C14−C15 stretching vibration, while the 1149 $cm^{-1}$ band is difficult to identify at present. The downshift of the C14−C15 stretching vibration from 1196 to 1189 $cm^{-1}$ upon formation of $ASR_K$ suggests that the retinal configuration is 13-cis in $ASR_K$. Splitting into two negative bands at 1174 and 1167 $cm^{-1}$ may suggest the presence of a positive band at 1171 $cm^{-1}$, which can be assigned to the C10−C11 stretching vibration.

The H−D exchangeable band at 1255 $cm^{-1}$ was assigned to one of the modes containing the N−H in-plane bending vibration of the Schiff base of BR (*24*), while similar negative bands appear at 1249 $cm^{-1}$ in the spectra of ASR. The band disappearing upon hydration with $D_2O$ can be assigned to the modes of the Schiff base. The neighboring negative band at 1237 $cm^{-1}$ is also sensitive to deuteration and seen only in ASR, but its origin remains unknown. The result suggests that the hydrogen bonding environment of the Schiff base of ASR is similar to that of BR.

The difference spectra in the 1110−890 $cm^{-1}$ region are expanded in Figure 5. Hydrogen-out-of-plane (HOOP), N−D in-plane bending, and methyl rocking vibrations are observed here, and the presence of strong HOOP modes represents the distortion of the retinal molecule at the corresponding position. The most intense HOOP band in the $BR_K$ minus BR difference spectra (Figure 5b) was observed at 957 $cm^{-1}$ (in $H_2O$) and 951 $cm^{-1}$ (in $D_2O$), which were assigned to the C15−H HOOP vibration of $BR_K$ (*24*). The origins of the bands at 941, 962, and 974 $cm^{-1}$ remain unknown, but they are considered to be able to be assigned to HOOP vibrations. On the other hand, the weak negative band at 911 $cm^{-1}$ was assigned to the C15−H and N−H HOOP vibrations of the original state of BR (*25*). These results have been interpreted as an increase in the retinal distortion around the Schiff base upon the retinal isomerization in BR. In the case of ASR, similar but slightly upshifted bands were observed. The positive bands at 1001, 973, 968, and 957 $cm^{-1}$ of $ASR_K$ (Figure 5a) possibly correspond to those at 974, 962, 957, and 941 $cm^{-1}$ of $BR_K$, respectively (Figure 5b). The negative bands at 932 and 927 $cm^{-1}$ have probably the same origin as that at 911 $cm^{-1}$ in BR, which was assigned to the C15−H and N−H HOOP vibrations (*25*).

The negative band at 976 $cm^{-1}$ and the positive band at 969 $cm^{-1}$ in Figure 5b were assigned to the N−D in-plane bending vibrations of BR and $BR_K$, respectively (*24*). The 1009 $cm^{-1}$ band is insensitive to H−D exchange and was assigned to the methyl rocking vibration of the retinal in BR. The band at 1006 $cm^{-1}$ in Figure 5a can also be assigned to the methyl rocking vibration in ASR similarly. On the other hand, the bands at 1088 (−), 1080 (+), and 1025 (−) $cm^{-1}$ are highly characteristic of the $ASR_K$ minus ASR difference spectra, and never observed in other archaeal-type rhodopsins such as BR, *p*pR, and NR (*18*, *24*, *26*). According to the literature, the antisymmetric $NC_3$ stretchings of tertiary amines appear in the 1250−1000 $cm^{-1}$ region (*27*). Thus, these bands may originate from the skeletal vibrations of Pro206 as well as those at 1471 (+), 1457 (−), and 1451 (−) $cm^{-1}$ (Figure 3a).

C═N stretching vibrations of the protonated retinal Schiff base are observed in the 1650−1600 $cm^{-1}$ region (Figure 6). The C═N stretching vibrations are sensitive to H−D exchange, and the difference in frequency has been considered as the probe for its hydrogen bonding strength (*28*, *29*). Namely, the larger the difference is, the stronger the hydrogen bond is. The C═NH and C═ND stretching vibrations of BR were observed at 1641 and 1628 $cm^{-1}$, while those of $BR_K$ were at 1608 and 1606 $cm^{-1}$, respectively (*30*). The former difference in frequency is 13 $cm^{-1}$, and the latter is 2 $cm^{-1}$, suggesting that the protonated Schiff base forms a hydrogen bond in BR and is broken upon retinal isomerization. The C═N stretchings were observed at 1642 (C═NH) and 1624 $cm^{-1}$ (C═ND) in ASR, and its difference

is 18 $cm^{-1}$, suggesting that the hydrogen bonding strength is stronger than that of BR. On the other hand, it is difficult to assign the positive bands because of the more complicated spectral feature. There are two sets of candidates for the C═N stretching vibrations of $ASR_K$. One set is the bands at 1621 (C═NH) and 1610 $cm^{-1}$ (C═ND), while another set is the bands at 1600 (C═NH) and 1595 $cm^{-1}$ (C═ND). The differences in frequency are 11 and 5 $cm^{-1}$ for the former and latter, respectively. If the former is the case, the hydrogen bond may not be broken upon retinal isomerization in ASR. Conclusive assignment of the C═N stretching of $ASR_K$ needs stable isotope labeling on the Schiff base, which is for our future study. On the other hand, the N−D stretching vibration of the Schiff base in $D_2O$ provides another and more direct information about the hydrogen bond of the Schiff base as described below.

*Comparison of the C═O Stretching Vibrations of Carboxylate, Carbonyl, and Amide Groups of the Protein Moiety between ASR and BR*. In the $BR_K$ minus BR difference spectra (Figure 6b), the bands at 1742 and 1733 $cm^{-1}$ were assigned to the C═O stretching vibrations of the protonated Asp115, which are downshifted upon hydration with $D_2O$ (*31*). In contrast, there is no band in the same frequency region of the ASR spectra (Figure 6a), implying that Asp and Glu residues are located far from the retinal molecule even if they are protonated. ASR has a glutamine residue at the corresponding position of Asp115 in BR, whose vibrational bands are probably observed at 1698 (−) and 1694 (+) $cm^{-1}$ (Figure 6a). Similar bands were also observed at 1704 (−) and 1700 (+) $cm^{-1}$ in the difference spectra of *p*pR, which has an asparagine residue at the corresponding position (*32*). These observations suggest that the structural changes around Asp115 in BR are similar among ASR, BR, and *p*pR.

The band pairs at 1668 (−)/1664 (+) $cm^{-1}$ and at 1623 (+)/1617 (−) $cm^{-1}$ were assigned to the C═O stretching vibrations of amide I. The former was assigned to the amide I of $\alpha_{II}$ helix (*33*) and the latter to the amide I of Val49 (*34*). In the case of ASR, a band pair at 1679 (−)/1673 (+) $cm^{-1}$ could be similar in origin to the bands at 1668 (−)/1664 (+) $cm^{-1}$ in BR. It should be noted that the spectral changes of amide I vibrations at <1660 $cm^{-1}$ are much smaller in ASR than in BR, which is clearly seen in $D_2O$. This suggests that the structural changes of the peptide backbone in ASR are very small upon retinal isomerization. On the other hand, the structural perturbation of Pro206 was suggested for ASR.

*Comparison of the X−D Stretching Vibrations between ASR and BR*. X−D stretching vibrations of protein and water molecules appear in the 2750−1950 $cm^{-1}$ region (Figure 7). A spectral comparison between the samples hydrated with $D_2O$ and $D_2{}^{18}O$ identifies O−D stretching vibrations of water molecules which change their frequencies upon retinal photoisomerization. Green-labeled bands in Figure 7 can be assigned to the O−D stretching vibrations of water because of the isotope shift. In BR, six negative peaks at 2690, 2636, 2599, 2321, 2292, and 2171 $cm^{-1}$ were earlier assigned to vibrations of water molecules (Figure 7b) (*16*, *35*). The bands are widely distributed over the possible frequency range for stretching vibrations of water. Since the frequencies of the negative peaks at 2321, 2292, and 2171 $cm^{-1}$ are much lower than those of fully hydrated tetrahedral water molecules (*35*),

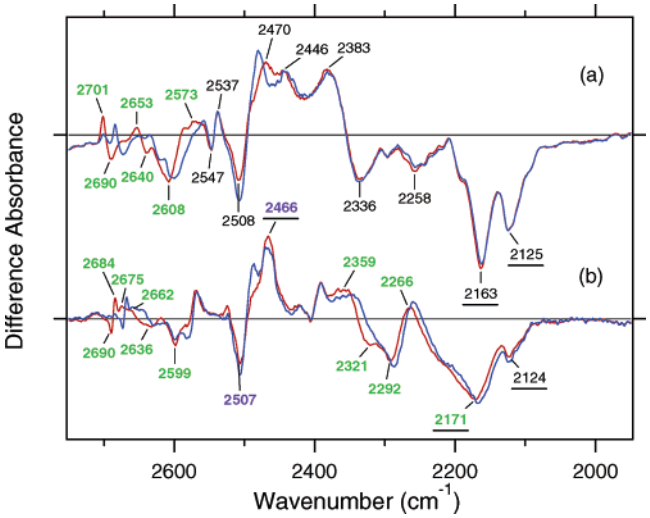


FIGURE 7: Comparison with the difference infrared spectra of ASR (a) and BR (b) hydrated with $D_2O$ (red lines) or $D_2{}^{18}O$ (blue lines) in the 2730−1950 $cm^{-1}$ region. Green-labeled frequencies correspond to those identified as water stretching vibrations. Purple-labeled frequencies are O−D stretches of Thr89 (*38*, *39*), while underlined frequencies are N−D stretches of the Schiff base (*30*). The spectrum in panel b is reproduced from Tanimoto et al. (*16*), where the sample window is tilted by 53.5°. One division of the *y*-axis corresponds to 0.0007 absorbance unit.

the hydrogen bonds of those water molecules must be very strong, possibly indicating their association with negative charges. Indeed, we assigned the 2171 $cm^{-1}$ band to the O−D group of a water molecule associated with deprotonated Asp85 (*15*). This water molecule, called water 402 in the crystal structure of BR (PDB entry 1C3W), is located between the Schiff base and Asp85 (Figure 1). A previous QM/MM calculation of the Schiff base region of BR also supported the existence of an extremely strong hydrogen bond between water 402 and Asp85 (*36*). Water stretching vibrations of $BR_K$ tend to be higher in frequency, implying that the overall hydrogen bonding becomes weaker upon photoisomerization.

In contrast, interestingly, only three negative peaks at 2690, 2640, and 2608 $cm^{-1}$ could be assigned to the O−D stretching vibrations of water in ASR (Figure 7a). The bands at 2701, 2653, and 2573 $cm^{-1}$ were assigned as water stretching vibrations of $ASR_K$. It should be emphasized that there are no water bands in the <2400 $cm^{-1}$ region, which is a significant difference from the published results for BR and *p*pR. In the case of *p*pR, two pairs of peaks were observed in the <2400 $cm^{-1}$ region, located at 2369 (+)/2307 (−) $cm^{-1}$ and at 2274 (+)/2215 (−) $cm^{-1}$ (*37*). Since ASR has a bridged water molecule between the Schiff base and Asp75 (Figure 1) as well as BR and *p*pR, one may expect similar water bands at <2400 $cm^{-1}$. However, that is not the case for ASR. We will discuss the structural reason for the lack of strongly hydrogen bonded water molecules below.

The frequency region shown in Figure 7 also contains X−D stretching vibrations other than water molecules. In the $BR_K$ minus BR spectrum, the bands at 2507 (−)/2466 (+) $cm^{-1}$ labeled in purple and the underlined bands at 2466 (+), 2171 (−), and 2124 (−) $cm^{-1}$ were assigned to the O−D stretching vibrations of Thr89 (*38*, *39*) (the corresponding residue in ASR is Thr79) and the N−D stretching vibrations of the retinal Schiff base (*30*), respectively. Thus, the

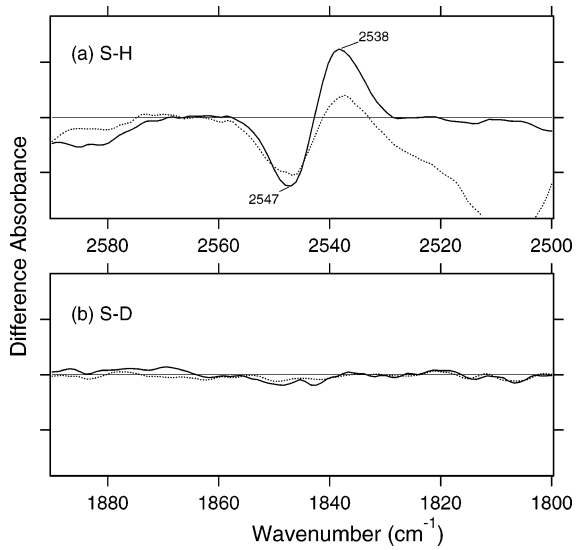


FIGURE 8: $ASR_K$ minus ASR spectra in the 2590−2500 $cm^{-1}$ (top panel) and 1890−1800 $cm^{-1}$ (bottom panel) region, which correspond to S−H and S−D stretching vibrations of cysteine residues, respectively. The sample was hydrated with $H_2O$ (—) or $D_2O$ (···). One division of the *y*-axis corresponds to 0.0001 absorbance unit.

negative 2171 $cm^{-1}$ band contains both the O−D stretch of water and the N−D stretch of the Schiff base. In the $ASR_K$ minus ASR spectrum, there are 10 bands other than water bands: 2547 (−), 2537 (+), 2508 (−), 2470 (−), 2446 (+), 2383 (+), 2336 (−), 2258 (−), 2163 (−), and 2125 (−) $cm^{-1}$. The bands at 2547 (−)/2537 (+) $cm^{-1}$ are attributed to the H−D unexchangeable S−H stretching vibration of a cysteine residue as described below. The bands at 2508 (−)/2470 (+) $cm^{-1}$ can be assigned to the O−D stretching vibrations of Thr79 in analogy to BR. The O−D frequencies of Thr79 in ASR and $ASR_K$ (2508 and 2470 $cm^{-1}$) are almost identical to those of Thr89 in BR and $BR_K$ (2507 and 2466 $cm^{-1}$), respectively, indicating that the strength of hydrogen bonding between Thr79 and Asp75 is identical to that between Thr89 and Asp85 in BR.

Though not assigned directly by use of the labeled protein, the bands at 2163 and 2125 $cm^{-1}$ are likely to originate from N−D stretching of the Schiff base, whose frequencies are very similar to those in BR (2171 and 2124 $cm^{-1}$). This fact indicates similar hydrogen bonding strengths between ASR and BR. The slightly lower frequency of the strong band (2163 $cm^{-1}$ in ASR and 2171 $cm^{-1}$ in BR) may correspond to the results obtained for the C═N stretching vibrations as shown before (Figure 6). The analysis of the C═N stretching vibrations of $ASR_K$ suggested two possibilities for the hydrogen bonding strength of the Schiff base. Figure 7a clearly shows the presence of the negative bands at 2163 and 2125 $cm^{-1}$, implying that the N−D stretch is upshifted in $ASR_K$. We infer that one of the bands at 2470, 2446, and 2383 $cm^{-1}$ can be assigned to the N−D stretch in $ASR_K$. Thus, we can safely conclude that the hydrogen bond of the Schiff base in ASR becomes much weaker upon retinal photoisomerization as well as in BR.

*S−H Stretching Vibrations of the Cysteine Residues.* Figure 8 shows the $ASR_K$ minus ASR spectra in the 2590−2500 $cm^{-1}$ (top panel) and 1890−1800 $cm^{-1}$ (bottom panel) regions, which correspond to S−H and S−D stretching vibrations of cysteine residues, respectively. There is a negative band at 2547 $cm^{-1}$ and a positive band at 2538 $cm^{-1}$, while no band is observed in the S−D stretching upon hydration with $D_2O$. In fact, S−H stretching vibrations in $D_2O$ are observed in Figure 7a (2547 and 2537 $cm^{-1}$). The S−H stretching frequency of cysteine appears in the 2580−2525 $cm^{-1}$ region. Thus, the frequency change from 2547 to 2538 $cm^{-1}$ suggests that the cysteine forms a considerably strong hydrogen bond upon retinal isomerization. The H−D unexchangeable nature of the cysteine S−H group presumably originates from either the hydrophobic environment or the strong hydrogen bond.

The lower-frequency shift in ASR is the opposite of the cysteine signal in the $NR_K$ minus NR spectra (*26*). In addition, the H−D exchange is different between ASR and NR. These facts suggest that the cysteine residues are located in different environments and their hydrogen bonds change differently. There are three cysteine residues in ASR, Cys134 and Cys137 in helix E and Cys203 in helix G. All of them are not conserved in archaeal-type rhodopsin, but Cys134 and Cys137 are located at a position similar to that of Cys170 in NR, which is conserved in halorhodopsin. The X-ray crystal structure of ASR also revealed that only the S−H group of Cys203 is directed to the inside of the protein. From these results, the observed band can be assigned to the S−H stretching of Cys203.

## DISCUSSION

In this study, we measured the $ASR_K$ minus ASR spectra by means of low-temperature FTIR spectroscopy. For this aim, ASR was expressed in *E. coli*, and the wild-type protein was reconstituted into PC liposomes. It is noted that the ASR molecule is not embedded in the native membrane, which could modify the FTIR spectra. For instance, H−D exchange may be different between PC liposomes and the native membrane, which should be elucidated in the future. However, this study focuses the structural changes near the retinal upon photoisomerization, and the light-induced difference FTIR spectra are not significantly affected by different lipid environments.

Despite the presence of the 13-cis form, the obtained spectra predominantly originate from the photoreaction of the all-trans form, and the spectra were compared with those of BR. These results clearly show that the all-trans to 13-cis photoisomerization takes place in ASR like in BR, though the C−C stretching and HOOP vibrations are somehow different. The protonated Schiff base forms a strong hydrogen bond in ASR presumably with the bridged water (Figure 1), and the hydrogen bond is cleaved by the rotation of the N−H (N−D) group, as in BR. We also observed S−H stretches of a cysteine residue which is insensitive to hydration with $D_2O$.

We observed the small bands of amide I, and large bands that can be ascribed to imide II [1471 (+), 1457 (−), and 1451 (−) $cm^{-1}$] and $NC_3$ [1088 (−) and 1080 (+) $cm^{-1}$] stretchings of proline residues. Previous resonance Raman spectroscopic study showed that the imide II vibration of the X−Pro bond appears at around 1450 $cm^{-1}$ (*40*). BR has three Pro residues in the transmembrane region, Pro50, Pro91, and Pro186 (Figure 2). The previous FTIR study suggested that the environment around these proline residues changes upon retinal isomerization via observation of the isotope effect of [$^{15}$N]proline in the 1450−1420 $cm^{-1}$ region.

(*41*). It should be noted that spectral changes are much smaller in BR than in ASR in this frequency region. In the case of ASR, there is an additional proline to the conserved three Pro residues (Figure 2). It is Pro206, a corresponding residue of Asp212 in BR (Figure 1). Figure 1 shows that the peptide C═O group of Pro206 forms a hydrogen bond with the peptide amide (N−H group) of Lys210, which connects a retinal chromophore. Thus, retinal photoisomerization strongly perturbs the peptide C−N bond of Pro206 in ASR, presumably leading to the appearance of these unusually intense bands in the 1500−1450 $cm^{-1}$ region. It should be noted, however, that we can conclude this argument only when these bands are assigned by use of [$^{15}$N]-proline-labeled ASR, which is now in progress.

A significant difference was seen for water bands between ASR and BR. We have so far observed the O−D stretching vibrations of water molecules under strongly hydrogen bonded conditions in the $BR_K$ minus BR and *p*$R_K$ minus *p*R difference spectra (*16*, *35*, *37*). The X-ray crystal structures of BR and *p*R reported the presence of a bridged water molecule between the Schiff base and its counterion (Asp85 in BR and Asp75 in *p*R) (*42*−*44*). Therefore, the hydrogen bond of the water is expected to be strong, and such strongly hydrogen bonded water molecules were observed in the FTIR studies. The water molecules possess O−D stretches at 2400−2100 $cm^{-1}$ in $D_2O$ (*13*, *17*). Since ASR has a bridged water molecule between the Schiff base and Asp75 (Figure 1) as well as BR and *p*R, one may expect similar water bands at <2400 $cm^{-1}$. However, that was not the case for ASR. Therefore, the structural reason for the lack of strongly hydrogen bonded water molecules has to be explained on the basis of the structural background. Since both structures of ASR and BR are known (Figure 1), we will try to explain the reason here.

Our analysis of the Schiff base mode (C═N stretch and N−D stretch) in ASR showed that the hydrogen bonding strength of the Schiff base is similar in ASR and BR. This observation is consistent with the similar distance between the Schiff base nitrogen and water oxygen (2.6 Å for ASR and 2.9 Å for BR). A slightly stronger hydrogen bond in ASR than in BR is also consistent with the distance that is shorter in ASR. In contrast, water bands in ASR were entirely different from those in BR, although the distance between the water oxygen and the oxygen of the counterion are similar (2.7 Å for ASR and 2.6 Å for BR). The O−D stretch of the bridged water in BR is located at 2171 $cm^{-1}$ (Figure 7b), whereas that in ASR is probably one of the bands at 2690, 2640, and 2608 $cm^{-1}$ (Figure 7a). How is such difference observed between ASR and BR? It may be explained by the difference in the geometry of the hydrogen bond. Figure 9 shows that the $N-O_{water}-O_{Asp75}$ (the Schiff base nitrogen, the water oxygen, and the oxygen of Asp75, respectively) angle in ASR is 83°. The corresponding $N-O_{water}-O_{Asp85}$ angle in BR is 106° (Figure 9). As the consequence, if the water oxygen fully accepts the hydrogen bond of the Schiff base, the O−H group of water points toward the oxygen of Asp85 in BR, but not toward that of Asp75 in ASR (Figure 9). Such a small difference in angle possibly determines the hydrogen bonding strength of water molecules.

On the basis of our FTIR studies of BR mutants and other rhodopsins, we have found an interesting correlation between

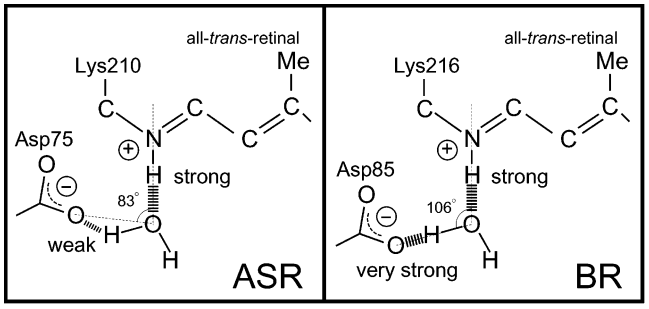


FIGURE 9: Schematic drawing of hydrogen bonds of the water molecule located between the protonated Schiff base and its counterion. A part of all-trans retinal is depicted, and the *β*-ionone ring and ethylenic part from C6 to C12 are omitted. The numbers are the angle of the N−O−O atoms derived from the crystal structures of ASR and BR (PDB entries 1XIO and 1C3W, respectively). Hydrogen bonds are represented as dashed lines with their strength.

strongly hydrogen bonded water molecules and proton pump activity. Among various BR mutant proteins we have studied, only D85N and D212N lack strongly hydrogen bonded water molecules. Other BR mutants possess their O−D stretches at <2400 $cm^{-1}$, which include T46V, R82Q, R82Q/D212N, T89A, D96N, D115N, Y185F, and E204Q (*45*). Among these mutants, only D85N and D212N do not pump protons. Therefore, strongly hydrogen bonded water molecules are only found in the proteins exhibiting proton pumping activities. The correlation between proton pumping activity and strongly hydrogen bonded water molecules is true not only for BR mutants but also for various rhodopsins. Whether rhodopsins possess strongly hydrogen bonded water molecules has been examined systematically. We found that BR and *pharaonis* phoborhodopsin (*16*, *35*, *37*), both of which pump protons, possess such water molecules (O−D stretch at <2400 $cm^{-1}$ in $D_2O$). In contrast, strongly hydrogen bonded water molecules were not observed for halorhodopsin (*46*), *Neurospora* rhodopsin (*26*), and bovine rhodopsin (*47*). It is known that none of them pumps protons. Such comprehensive studies of archaeal and visual rhodopsins have thus revealed that strongly hydrogen bonded water molecules are only found in the proteins exhibiting proton pumping activities. Taken together, these results for ASR suggest that the strong hydrogen bonds of water molecules and their transient weakening may be essential for the proton pumping function of rhodopsins.

## ACKNOWLEDGMENT

We thank Drs. Shimono and Sudo for providing a procedure for the *E. coli* expression system.

## REFERENCES

1. Sasaki, J., and Spudich, J. L. (2000) Proton transport by sensory rhodopsins and its modulation by transducer-binding, *Biochim. Biophys. Acta 1460*, 230−239.
2. Kamo, N., Shimono, K., Iwamoto, M., and Sudo, Y. (2001) Photochemistry and photoinduced proton-transfer by pharaonis phoborhodopsin, *Biochemistry (Moscow) 66*, 1277−1282.
3. Bieszke, J. A., Braun, E. L., Bean, L. E., Kang, S., Natvig, D. O., and Borkovich, K. A. (1999) The nop-1 gene of *Neurospora crassa* encodes a seven transmembrane helix retinal-binding protein homologous to archaeal rhodopsins, *Proc. Natl. Acad. Sci. U.S.A. 96*, 8034−8039.

4. Sineshchekov, O. A., Jung, K. H., and Spudich, J. L. (2002) Two rhodopsins mediate phototaxis to low- and high-intensity light in *Chlamydomonas reinhardtii*, *Proc. Natl. Acad. Sci. U.S.A. 99*, 8689−8694.
5. Nagel, G., Ollig, D., Fuhrmann, M., Kateriya, S., Musti, A. M., Bamberg, E., and Hegemann, P. (2002) Channelrhodopsin-1: A light-gated proton channel in green algae, *Science 296*, 2395−2398.
6. Okamoto, O. K., and Hastings, J. W. (2003) Novel dinoflagellate clock-related genes identified through microarray analysis, *J. Phycol. 39*, 519−526.
7. Jung, K. H., and Spudich, J. L. (2004) Microbial rhodopsins: Transport and sensory proteins throughout the three domains of life, in *CRC Handbook of Organic Photochemistry and Photobiology* (Horspool, W. M., and Lenci, F., Eds.) 2nd ed., Section II Photobiology, pp 124/1−124/11, CRC Press, Boca Raton, FL.
8. de la Torre, J. R., Christianson, L. M., Beja, O., Suzuki, M. T., Karl, D. M., Heidelberg, J., and DeLong, E. F. (2003) Proteorhodopsin genes are distributed among divergent marine bacterial taxa, *Proc. Natl. Acad. Sci. U.S.A. 100*, 12830−12835.
9. Beja, O., Aravind, L., Koonin, E. V., Suzuki, M. T., Hadd, A., Nguyen, L. P., Jovanovich, S. B., Gates, C. M., Feldman, R. A., Spudich, J. L., Spudich, E. N., and DeLong, E. F. (2000) Bacterial rhodopsin: Evidence for a new type of phototrophy in the sea, *Science 289*, 1902−1906.
10. Jung, K. H., Trivedi, V. D., and Spudich, J. L. (2003) Demonstration of a sensory rhodopsin in eubacteria, *Mol. Microbiol. 47*, 1513−1522.
11. Vogeley, L., Sineshchekov, O. A., Trivedi, V. D., Sasaki, J., Spudich, J. L., and Luecke, H. (2004) *Anabaena* sensory rhodopsin: A photochromic color sensor at 2.0 Å, *Science 306*, 1390−1393.
12. Iwamoto, M., Shimono, K., Sumi, M., and Kamo, N. (1999) Positioning proton-donating residues to the Schiff-base accelerates the M-decay of *pharaonis* phoborhodopsin expressed in *Escherichia coli*, *Biophys. Chem. 79*, 187−192.
13. Kandori, H. (2004) Hydration switch model for the proton transfer in the Schiff base region of bacteriorhodopsin, *Biochim. Biophys. Acta 1658*, 72−79.
14. Kandori, H. (2000) Role of internal water molecules in bacteriorhodopsin, *Biochim. Biophys. Acta 1460*, 177−191.
15. Shibata, M., Tanimoto, T., and Kandori, H. (2003) Water Molecules in the Schiff Base Region of Bacteriorhodopsin, *J. Am. Chem. Soc. 125*, 13312−13313.
16. Tanimoto, T., Furutani, Y., and Kandori, H. (2003) Structural changes of water in the Schiff base region of bacteriorhodopsin: Proposal of a hydration switch model, *Biochemistry 42*, 2300−2306.
17. Furutani, Y., Shibata, M., and Kandori, H. (2005) Strongly hydrogen-bonded water molecules in the Schiff base region of rhodopsins, *Photochem. Photobiol. Sci.* (in press).
18. Kandori, H., Shimono, K., Sudo, Y., Iwamoto, M., Shichida, Y., and Kamo, N. (2001) Structural changes of *pharaonis* phoborhodopsin upon photoisomerization of the retinal chromophore: Infrared spectral comparison with bacteriorhodopsin, *Biochemistry 40*, 9238−9246.
19. Aton, B., Doukas, A. G., Callender, R. H., Becher, B., and Ebrey, T. G. (1977) Resonance Raman studies of the purple membrane, *Biochemistry 16*, 2995−2999.
20. Rothschild, K. J., Bousche, O., Braiman, M. S., Hasselbacher, C. A., and Spudich, J. L. (1988) Fourier transform infrared study of the halorhodopsin chloride pump, *Biochemistry 27*, 2420−2424.
21. Smith, S. O., Braiman, M. S., Myers, A. B., Pardoen, J. A., Courtin, J. M. L., Winkel, C., Lugtenburg, J., and Mathies, R. A. (1987) Vibrational analysis of the all-trans-retinal chromophore in light-adapted bacteriorhodopsin, *J. Am. Chem. Soc. 109*, 3108−3125.
22. Braiman, M., and Mathies, R. (1982) Resonance Raman spectra of bacteriorhodopsin's primary photoproduct: Evidence for a distorted 13-cis retinal chromophore, *Proc. Natl. Acad. Sci. U.S.A. 79*, 403−407.
23. Roepe, P. D., Ahl, P. L., Herzfeld, J., Lugtenburg, J., and Rothschild, K. J. (1988) Tyrosine protonation changes in bacteriorhodopsin. A Fourier transform infrared study of BR548 and its primary photoproduct, *J. Biol. Chem. 263*, 5110−5117.
24. Maeda, A., Sasaki, J., Pfefferle, J. M., Shichida, Y., and Yoshizawa, T. (1991) Fourier transform infrared spectral studies on the Schiff base mode of all-trans bacteriorhodopsin and its photointermediates, K and L, *Photochem. Photobiol. 54*, 911−921.
25. Maeda, A., Balashov, S. P., Lugtenburg, J., Verhoeven, M. A., Herzfeld, J., Belenky, M., Gennis, R. B., Tomson, F. L., and Ebrey, T. G. (2002) Interaction of internal water molecules with the schiff base in the L intermediate of the bacteriorhodopsin photocycle, *Biochemistry 41*, 3803−3809.
26. Furutani, Y., Bezerra, A. G., Jr., Waschuk, S., Sumii, M., Brown, L. S., and Kandori, H. (2004) FTIR spectroscopy of the K photointermediate of *Neurospora* rhodopsin: Structural changes of the retinal, protein, and water molecules after photoisomerization, *Biochemistry 43*, 9636−9646.
27. Lin-Vien, D., Colthup, N. B., Fateley, W. G., and Grasselli, J. G. (1991) *The Handbook of Infrared and Raman Characteristic Frequencies of Organic Molecules*, Academic Press, New York.
28. Rodman-Gilson, H. S., Honig, B., Croteau, A., Zarrilli, G., and Nakanishi, K. (1988) Analysis of the factors that influence the C═N stretching frequency of polyene Schiff bases. Implications for bacteriorhodopsin and rhodopsin, *Biophys. J. 53*, 261−269.
29. Baasov, T., Friedman, N., and Sheves, M. (1987) Factors affecting the C═N stretching in protonated retinal Schiff base: A model study for bacteriorhodopsin and visual pigments, *Biochemistry 26*, 3210−3217.
30. Kandori, H., Belenky, M., and Herzfeld, J. (2002) Vibrational frequency and dipolar orientation of the protonated Schiff base in bacteriorhodopsin before and after photoisomerization, *Biochemistry 41*, 6026−6031.
31. Mogi, T., Stern, L. J., Marti, T., Chao, B. H., and Khorana, H. G. (1988) Aspartic acid substitutions affect proton translocation by bacteriorhodopsin, *Proc. Natl. Acad. Sci. U.S.A. 85*, 4148−4152.
32. Kandori, H., Shimono, K., Shichida, Y., and Kamo, N. (2002) Interaction of Asn105 with the retinal chromophore during photoisomerization of *pharaonis* phoborhodopsin, *Biochemistry 41*, 4554−4559.
33. Krimm, S., and Dwivedi, A. M. (1982) Infrared spectrum of the purple membrane: Clue to a proton conduction mechanism? *Science 216*, 407−408.
34. Yamazaki, Y., Tuzi, S., Saito, H., Kandori, H., Needleman, R., Lanyi, J. K., and Maeda, A. (1996) Hydrogen bonds of water and C═O groups coordinate long-range structural changes in the L photointermediate of bacteriorhodopsin, *Biochemistry 35*, 4063−4068.
35. Kandori, H., and Shichida, Y. (2000) Direct Observation of the Bridged Water Stretching Vibrations Inside a Protein, *J. Am. Chem. Soc. 122*, 11745−11746.
36. Hayashi, S., Tajkhorshid, E., Kandori, H., and Schulten, K. (2004) Role of hydrogen-bond network in energy storage of bacteriorhodopsin's light-driven proton pump revealed by ab initio normal-mode analysis, *J. Am. Chem. Soc. 126*, 10516−10517.
37. Kandori, H., Furutani, Y., Shimono, K., Shichida, Y., and Kamo, N. (2001) Internal water molecules of *pharaonis* phoborhodopsin studied by low-temperature infrared spectroscopy, *Biochemistry 40*, 15693−15698.
38. Kandori, H., Yamazaki, Y., Shichida, Y., Raap, J., Lugtenburg, J., Belenky, M., and Herzfeld, J. (2001) Tight Asp-85−Thr-89 association during the pump switch of bacteriorhodopsin, *Proc. Natl. Acad. Sci. U.S.A. 98*, 1571−1576.
39. Kandori, H., Kinoshita, N., Yamazaki, Y., Maeda, A., Shichida, Y., Needleman, R., Lanyi, J. K., Bizounok, M., Herzfeld, J., Raap, J., and Lugtenburg, J. (1999) Structural change of threonine 89 upon photoisomerization in bacteriorhodopsin as revealed by polarized FTIR spectroscopy, *Biochemistry 38*, 9676−9683.
40. Takeuchi, H., and Harada, I. (1990) Ultraviolet resonance Raman spectroscopy of X-proline bonds: A new marker band of hydrogen bonding at the imide C═O site, *J. Raman Spectrosc. 21*, 509−515.
41. Rothschild, K. J., He, Y. W., Gray, D., Roepe, P. D., Pelletier, S. L., Brown, R. S., and Herzfeld, J. (1989) Fourier transform infrared evidence for proline structural changes during the bacteriorhodopsin photocycle, *Proc. Natl. Acad. Sci. U.S.A. 86*, 9832−9835.

42. Royant, A., Nollert, P., Edman, K., Neutze, R., Landau, E. M., Pebay-Peyroula, E., and Navarro, J. (2001) X-ray structure of sensory rhodopsin II at 2.1-Å resolution, *Proc. Natl. Acad. Sci. U.S.A. 98*, 10131−10136.
43. Luecke, H., Schobert, B., Richter, H. T., Cartailler, J. P., and Lanyi, J. K. (1999) Structure of bacteriorhodopsin at 1.55 Å resolution, *J. Mol. Biol. 291*, 899−911.
44. Luecke, H., Schobert, B., Lanyi, J. K., Spudich, E. N., and Spudich, J. L. (2001) Crystal structure of sensory rhodopsin II at 2.4 Å: Insights into color tuning and transducer interaction, *Science 293*, 1499−1503.
45. Shibata, M., and Kandori, H. (2005) FTIR studies of internal water molecules in the Schiff base region of bacteriorhodopsin, *Biochemistry 44*, 7406−7413.
46. Shibata, M., Muneda, N., Ihara, K., Sasaki, T., Demura, M., and Kandori, H. (2004) Internal water molecules of light-driven chloride pump proteins, *Chem. Phys. Lett. 392*, 330−333.
47. Furutani, Y., Shichida, Y., and Kandori, H. (2003) Structural changes of water molecules during the photoactivation processes in bovine rhodopsin, *Biochemistry 42*, 9619−9625.
48. Guex, N., and Peitsch, M. C. (1997) SWISS-MODEL and the Swiss-PdbViewer: An environment for comparative protein modeling, *Electrophoresis 18*, 2714−2723.
49. Thompson, J. D., Higgins, D. G., and Gibson, T. J. (1994) CLUSTAL W: Improving the sensitivity of progressive multiple sequence alignment through sequence weighting, position-specific gap penalties and weight matrix choice, *Nucleic Acids Res. 22*, 4673−4680.
50. Kandori, H., Kinoshita, N., Shichida, Y., and Maeda, A. (1998) Protein structural changes in bacteriorhodopsin upon photoisomerization as revealed by polarized FTIR spectroscopy, *J. Phys. Chem. B 102*, 7899−7905.

BI050841O